Supporting Information

[Ru(bpy)$_2$(dppz)]$^{2+}$ encapsulated isostructural In-MOFs: a comparative study of their photoluminescence and photoredox catalytic activities

Jongseo Kim,[†] Chan Gu Kim,[†] Juwon Lee and Seong Huh[*]

Department of Chemistry and Protein Research Center for Bio-Industry, Hankuk University of Foreign Studies, Yongin 17035, Republic of Korea. E-mail: shuh@hufs.ac.kr

[†]These authors contributed equally to this work.

Experimental Procedures

Chemicals. All solvents are reagent grade and used as received unless otherwise noted. $Ru(bpy)_2Cl_2 \cdot xH_2O$ (Sigma-Aldrich), *N*,*N*-diethylformamide (DEF, TCI) and 1,1,2,2-tetrachloroethane (TCE, TCI) were used as received. 1,10-Phenanthroline-5,6-dione [1], dipyrido[3,2-a:2',3'-c]phenazine (dppz) [1], and $[Ru(bpy)_2(dppz)][BF_4]_2$ [1], InBTB [2], InTATB [3], and 2-phenyl-1,2,3,4-tetrahydroisoquinoline (THIQ) [4] were synthesized according to the literature method.

Encapsulation of $[Ru(bpy)_2(dppz)]^{2+}$ complex into In-MOF. $[Ru(bpy)_2(dppz)][BF_4]_2$ dissolved in 10 mL of acetonitrile (2 mM) containing 10 mg of as-prepared InBTB or InTATB were gently shaken for 5 days. $Ru(bpy)_2(dppz)$@InBTB and $Ru(bpy)_2(dppz)$@InTATB were retrieved by filtration, washed with ethanol, and dried in air. The final products in vials were kept in a desiccator before use.

General procedure for aza-Henry reaction. A suitable amount of THIQ was dissolved in 5 mL of reagent-grade nitromethane in 50 mL round-bottom flask. $[Ru(bpy)_2(dppz)][BF_4]_2$ or $Ru(bpy)_2(dppz)$@In-MOF equivalent to 2.5×10^{-3} mmol of $[Ru(bpy)_2(dppz)]^{2+}$ complex were added into the reaction mixture. After a small magnetic stir bar was added, the single-neck round-bottom flask was capped with a rubber septum with a pinhole by syringe needle. The reaction flask was placed at 10 cm from a 20 W fluorescent lamp.

Aza-Henry reaction with $Ru(bpy)_2(dppz)$@In-MOFs. Following the general procedure, THIQ (26.16 mg, 0.125 mmol) was used as a substrate and the reaction mixture was exposed

to light for 48 h. After reaction, $Ru(bpy)_2(dppz)$@In-MOF was separated by centrifugation. The supernatant was transferred to 250 mL round-bottom flask and residual solution was washed with $CHCl_3$. The reaction mixture was evaporated to dryness by a rotary evaporator, and dried under high vacuum. The residue was dissolved in a small amount of $CDCl_3$, and TCE (13.2 μL, 0.125 mmol) was added. The substrate conversion and product yield were measured by using ^1H NMR spectroscopy.

Aerobic oxidation of benzyl halides with $Ru(bpy)_2(dppz)$@In-MOFs. A benzyl halide of choice (0.2 mmol), 4-methoxypyridine (4 μL, 0.04 mmol), Li_2CO_3 (0.0148 g, 0.2 mmol) was dissolved in 1 mL of reagent-grade dimethylacetamide (DMA) in a 10 mL round-bottom flask. The $Ru(bpy)_2(dppz)$@In-MOF equivalent to 2.0×10^{-3} mmol of $[Ru(bpy)_2(dppz)]^{2+}$ was added into the reaction mixture. After a small magnetic stir bar was added, the round-bottom flask was capped with a rubber septum with a pinhole (syringe needle). The reaction flask was placed at 5 cm distance from a compact fluorescent lamp (20 W Cool White CFL, GE Edison). The reaction mixture was exposed to light for 48 h. After the reaction, the $Ru(bpy)_2(dppz)$@In-MOF was separated by centrifugation. DMA (9 mL) was added into the supernatant, and ethyl acetate (30 mL) and deionized water (30 mL) were also added. The organic phase was separated. The extraction was repeated three more times using ethyl acetate (50 mL). The combined organic phase was washed with a brine (25% NaCl) three times. The organic phase was dried using anhydrous $MgSO_4$. After filtration, the dried organic phase was evaporated to dryness by rotary evaporator and dried under high vacuum. The residue was dissolved in a small amount of $CDCl_3$, and TCE (21.1 μL, 0.2 mmol) was added. The substrate conversion and product yield were measured by ^1H NMR spectroscopy.

Instrumentation. NMR spectra were recorded using a Bruker Ascend 400 (400.13MHz for ^{1}H) spectrometer. The proton chemical shifts of the samples were calibrated with respect to the reference proton resonance signals occurring from the protic residues of the deuterated solvents. The elemental composition of the MOF sample was analyzed at the Organic Chemistry Research Center (Seoul, Korea). PXRD spectra were recorded on a Bruker D8 Focus diffractometer (40 kV, 30 mA, step size = 0.02°). UV-Vis spectra were collected by a Scinco S-3100 spectrophotometer. Solid-state fluorescence spectra were collected using a Hitachi F-4500 fluorescence spectrophotometer.

Cyclic voltammetry. Cyclic voltammetry (CV) was performed using a CompactStat potentiostat/galvanostat (Ivium Technologies, Netherlands). Cyclic voltammograms were recorded using a glassy carbon working electrode (CHI104, O.D. 6.35 mm, I.D. 3 mm, CH Instruments, USA), an Ag/AgCl reference electrode (RE-1B, ALS, Japan), and a Pt wire counter electrode in 0.1 M $TEABF_4$ acetonitrile solution. All measurements were conducted under an inert atmosphere by thoroughly bubbling nitrogen gas for 1 h prior to each session. A small amount of solid sample was directly put on a glassy carbon electrode, covered with a few drops of Nafion-117 solution (Sigma Aldrich), and dried at room temperature for 2 h. The voltage was applied in the following manner: 0 V → 2.5 V → −2.5 V → 0 V. The scan rate was 20 mV s^{-1}. The CV curves were cycled four times, and the second CV curve was used to calculate the redox potential. The third and fourth scans exhibited almost the same profiles as the second scan.

Photoluminescence lifetime measurements. Time-resolved photoluminescence (TRPL) imaging was performed using an inverted-type scanning confocal microscope (MicroTime-

200, Picoquant, Germany) with a 60× (water) objective. The measurements were performed at the Korea Basic Science Institute, Daegu Center. A single-mode pulsed diode laser (470 nm with ~30 ps pulse width and an average power of < 1 μW) was used as an excitation source. A dichroic mirror (490 DCXR, AHF), a long-pass filter (HQ500lp, AHF), and a single-photon avalanche diode (SPAD; PDM series, MPD) were used to collect the emission data from each sample. A time-correlated single-photon counting technique was used to count emitting photons. TRPL images with a dimension of 80 × 80 μm^2, which consisted of 200 × 200 pixels, were recorded using a time-tagged time-resolved (TTTR) data acquisition route. The acquisition time was 2 ms for each pixel. Exponential fittings for the obtained PL decays were performed using the Symphotime-64 software.

Table S1. Amplitude average PL lifetimes (τ) in ns. All measurements were performed in a solid state.

	Free ion	$Ru(bpy)_2(dppz)$@InBTB	$Ru(bpy)_2(dppz)$@InTATB
$[Ru(bpy)_2(dppz)][BF_4]_2$	21 ± 0.27	270 ± 1.8	254 ± 1.9

Table S2. The PL lifetime components (τ in ns) extracted from the curve fitting of decay profiles using suitable exponential models. The data for crystalline $[Ru(bpy)_2(dppz)]^{2+}$ ion is shown together. All measurements were performed in solid state.

	$[Ru(bpy)_2(dppz)][BF_4]_2$	$Ru(bpy)_2(dppz)$@InBTB	$Ru(bpy)_2(dppz)$@InTATB
τ_1	14 ± 0.48	659 ± 11	635 ± 7.1
τ_2	280 ± 13	270 ± 6.5	254 ± 4.2
τ_3	42 ± 1.6	37 ± 2	41 ± 2.3

Table S3. The redox potentials of $Ru(bpy)_2(dppz)$@In-MOFs in V (vs. SCE).

	$E_{1/2}$	$[Ru(bpy)_2(dppz)]^{2+}$[a]	$Ru(bpy)_2(dppz)$@ InBTB	$Ru(bpy)_2(dppz)$@ InTATB
Excited state	Ru^{III}/Ru^{II*}	-0.73	-0.71	-0.71
redox potentials[b]	Ru^{II*}/Ru^{I}	+1.05	+1.17	+1.17
Ground state	Ru^{III}/Ru^{II}	+1.29	+1.31	+1.31
redox potentials[c]	$Ru^{II}(dppz)/Ru^{II}(dppz^{\bullet-})$[d]	-0.97	-0.85	-0.85

[a] The excited state energy ($E_{0,0}$) of $[Ru(bpy)_2(dppz)]^{2+}$ complex was estimated based on literature value in CH_3CN (λ_{max} of emission spectrum = 615 nm; $E_{0,0} \approx 1240/615$ nm = 2.02 eV) [5]. [b] Excited state oxidation and reduction potentials were calculated according to the following relationships: $E_{1/2}(Ru^{III}/Ru^{II*}) \approx E_{1/2}(Ru^{III}/Ru^{II}) - E_{0,0}$ and $E_{1/2}(Ru^{II*}/Ru^{I}) \approx E_{1/2}(Ru^{II}/Ru^{I}) + E_{0,0}$ [6,7]. [c] Ground state half-wave potentials were obtained using cyclic voltammetry ($E_{1/2} = ½(E_{pa} + E_{pc})$). [d] This reduction process is ligand-centered rather than metal-centered.

Table S4. The product yields and selectivity of the oxidation of benzyl bromides by $Ru(bpy)_2(dppz)$@InBTB and $Ru(bpy)_2(dppz)$@InTATB.[a] The desired product yields are shown in bold numbers.

Substrates	Products		$Ru(bpy)_2(dppz)$@InBTB	$Ru(bpy)_2(dppz)$@InTATB
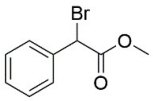	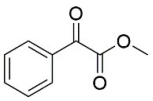	C	95	85
		Y	**66**	**64**
		S	69	75
		TON	66	64
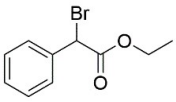	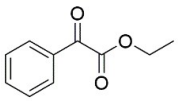	C	86	92
		Y	**68**	**68**
		S	79	74
		TON	68	68
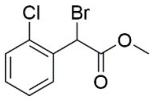	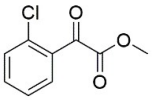	C	89	80
		Y	**68**	**60**
		S	76	75
		TON	68	60
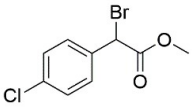	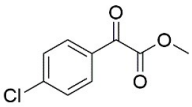	C	100	98
		Y	**79**	**71**
		S	79	72
		TON	79	71
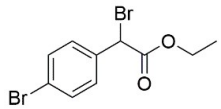	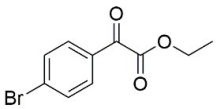	C	85	98
		Y	**85**	**90**
		S	100	92
		TON	85	90

[a] Reaction conditions: $Ru(bpy)_2(dppz)$@In-MOF (0.002 mmol based on $[Ru(bpy)_2(dppz)]^{2+}$); benzyl bromides (0.2 mmol); Li_2CO_3 (0.2 mmol); 4-methoxypyridine (0.04 mmol); dimethylacetamide (1 mL); fluorescent lamp irradiation for 48 h at RT. C = conversions (%); Y = desired product yields (%); S = selectivity defined by the following equation, [desired product yield/conversion]×100(%); TON = turnover number for desired product.

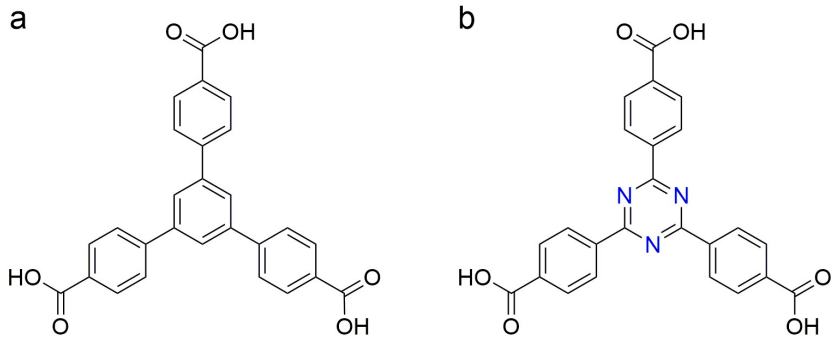

Fig. S1 The chemical structures of H_3BTB (a) and H_3TATB (b).

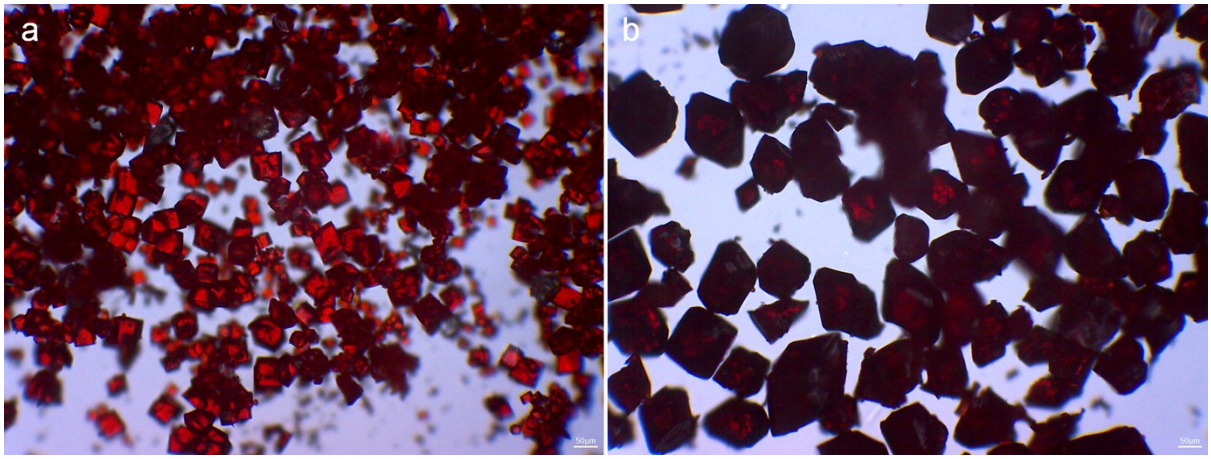

Fig. S2 Optical microscopic images of $Ru(bpy)_2(dppz)$@InBTB (a) and $Ru(bpy)_2(dppz)$@InTATB.

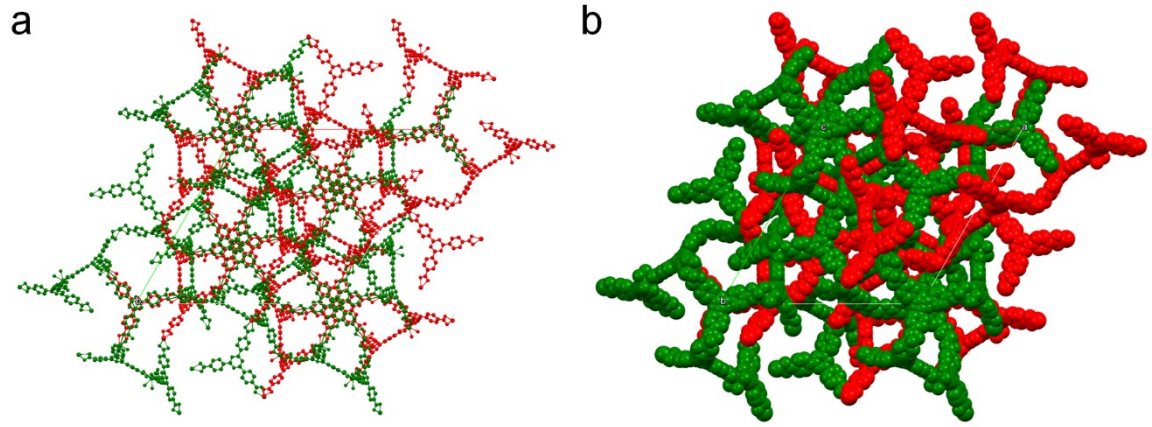

Fig. S3 The crystal structure of a doubly-interpenetrated InTATB framework shown in a ball-and-stick representation (a) and a CPK representation (b) along the *c*-axis. Hydrogen atoms, counter-cations, and solvent are omitted for clarity [3].

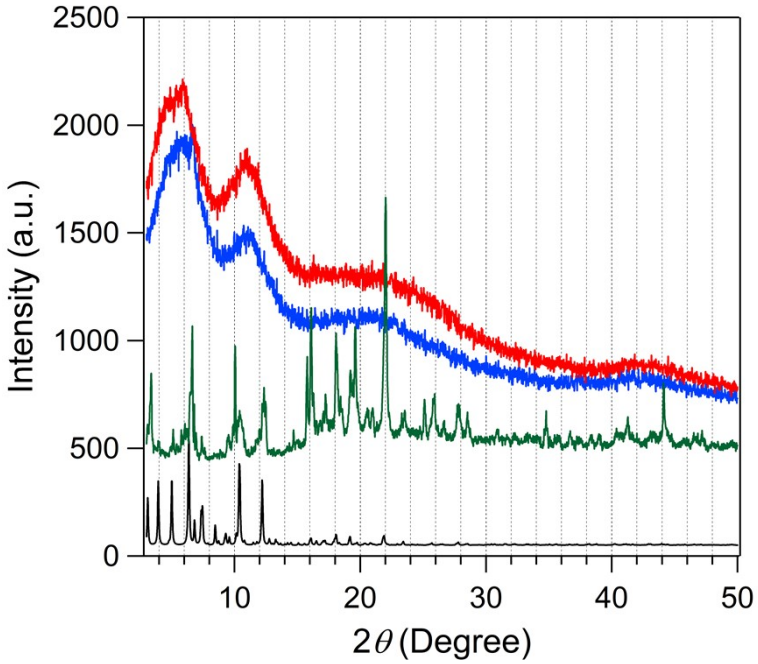

Fig. S4 The PXRD patterns of as-prepared InBTB (green), $Ru(bpy)_2(dppz)$@InBTB (blue) and $Ru(bpy)_2(dppz)$@InTATB (red). The simulated pattern of InBTB is shown in black. Because InBTB and InTATB are isostructural and exhibit nearly identical PXRD patterns, only the simulated data for InBTB is provided.

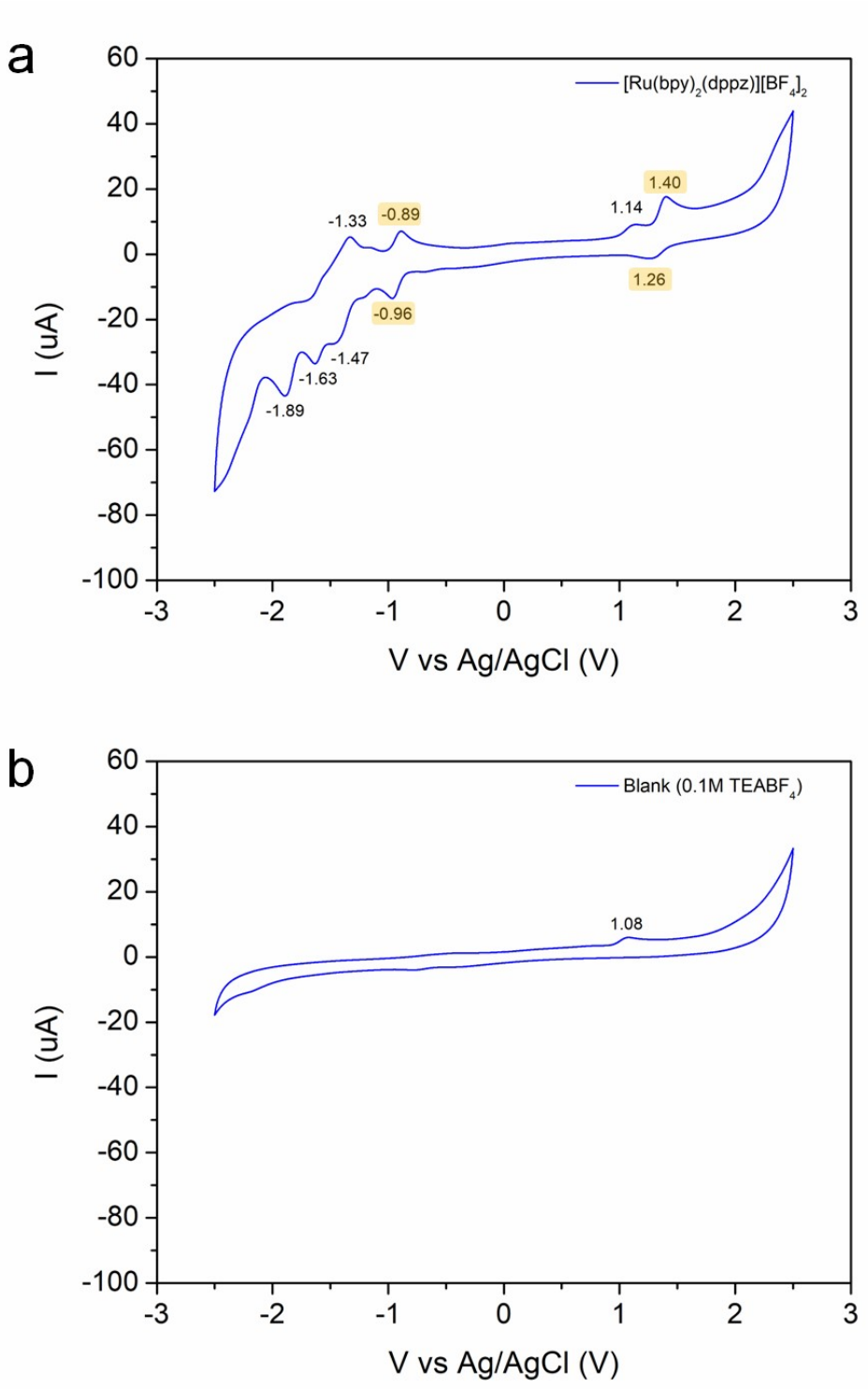

Fig. S5 The cyclic voltammograms of $[Ru(bpy)_2(dppz)][BF_4]_2$ in 0.1 M $TEABF_4$ acetonitrile solution (a) and the blank solution without Ru(II) complex (b). Both CV curves were obtained at a scan rate of 20 mV/s under an inert atmosphere. The first reduction and oxidation peaks of $[Ru(bpy)_2(dppz)][BF_4]_2$ are highlighted in orange in panel (a).

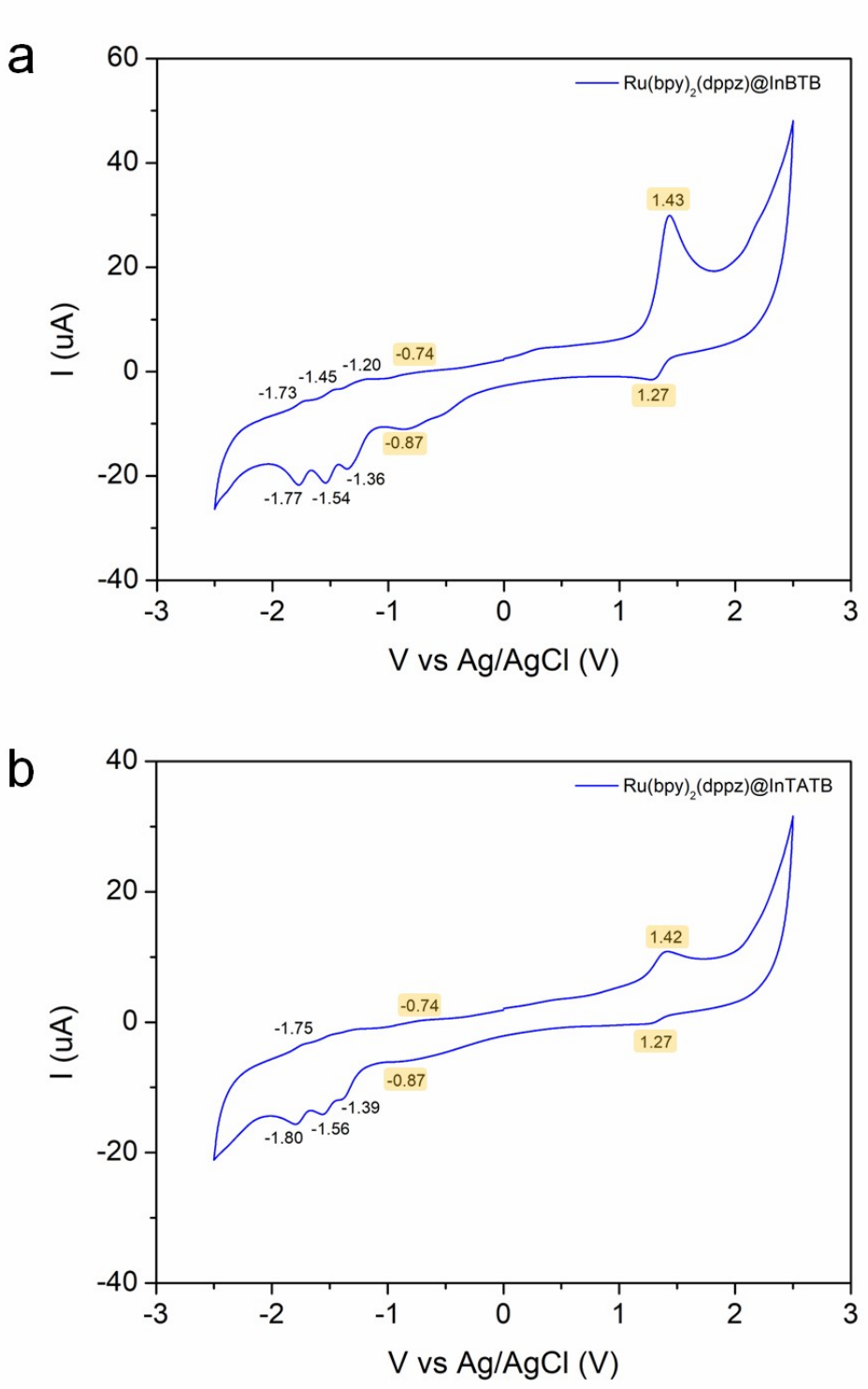

Fig. S6 The cyclic voltammograms of $Ru(bpy)_2(dppz)$@InBTB (a) and $Ru(bpy)_2(dppz)$@InTATB (b) in 0.1 M $TEABF_4$ acetonitrile solution. Both CV curves were obtained at a scan rate of 20 mV/s under an inert atmosphere. The first reduction and oxidation peaks are marked in orange.

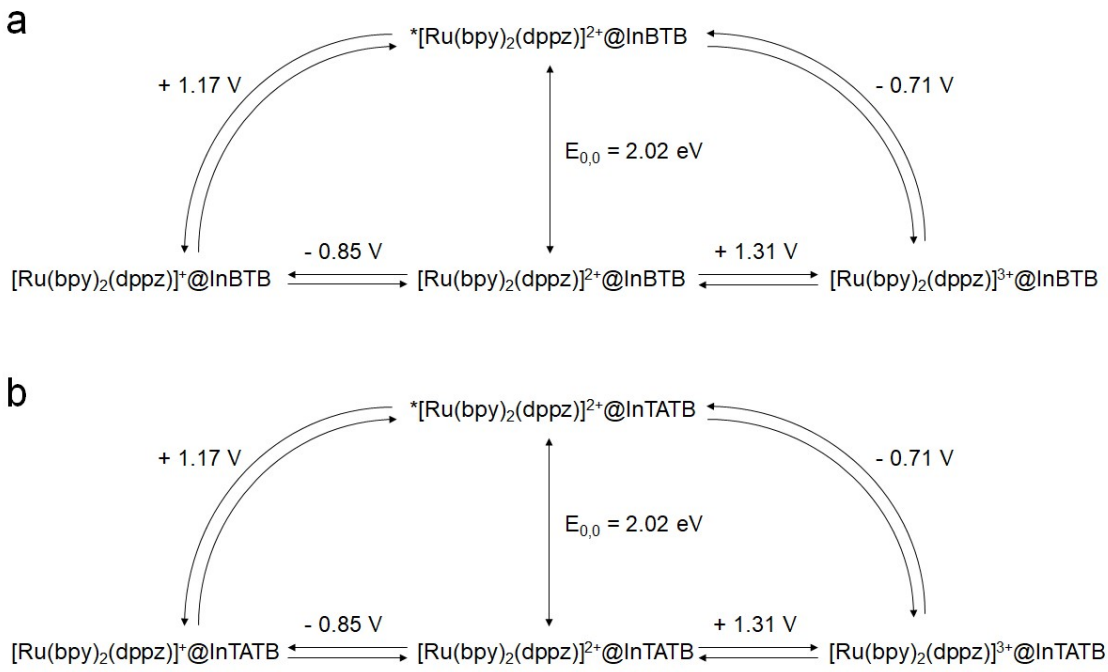

Fig. S7 The redox potential diagrams of ground state and excited state of $Ru(bpy)_2(dppz)$@InBTB (a) and $Ru(bpy)_2(dppz)$@InTATB (b).

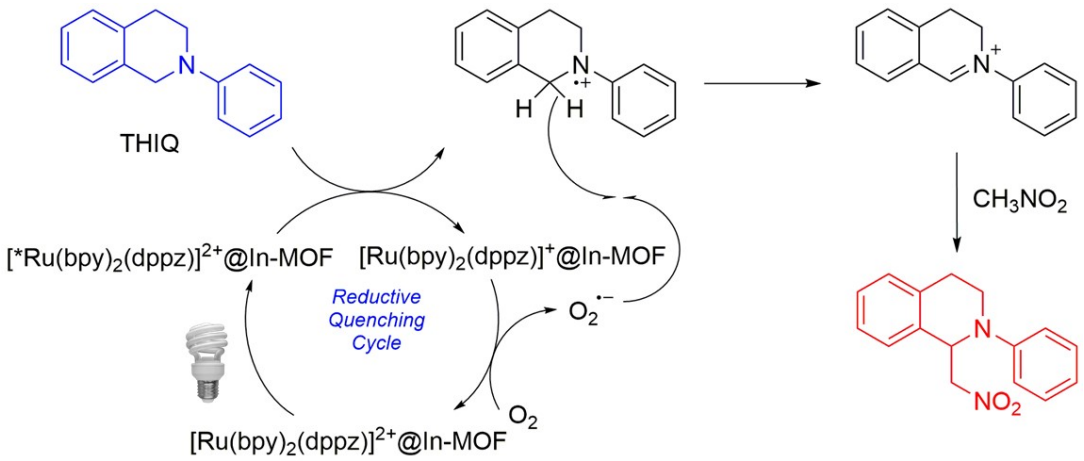

Fig. S8 A proposed reaction mechanism of the aza-Henry reaction between THIQ and nitromethane catalyzed by $Ru(bpy)_2(dppz)$@In-MOF [8].

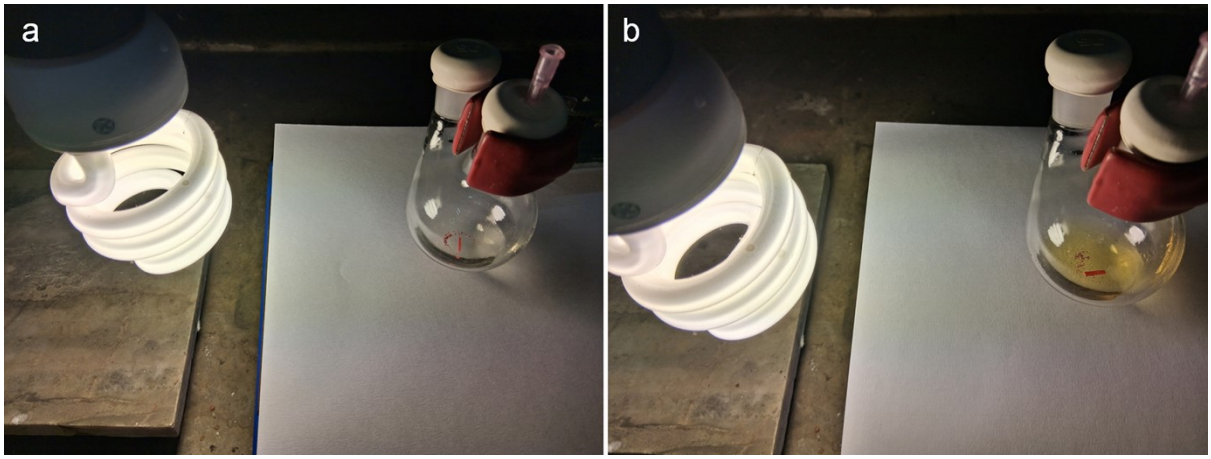

Fig. S9 Digital photographs of the reaction mixture taken before (a) and after (b) the aza-Henry reaction catalyzed by Ru(bpy)$_2$(dppz)@InTATB. A large red magnetic stirring bar is also shown. The orange color of the reaction mixture shown in panel (b) is partially attributed to the presence of the red-colored iminium intermediate.

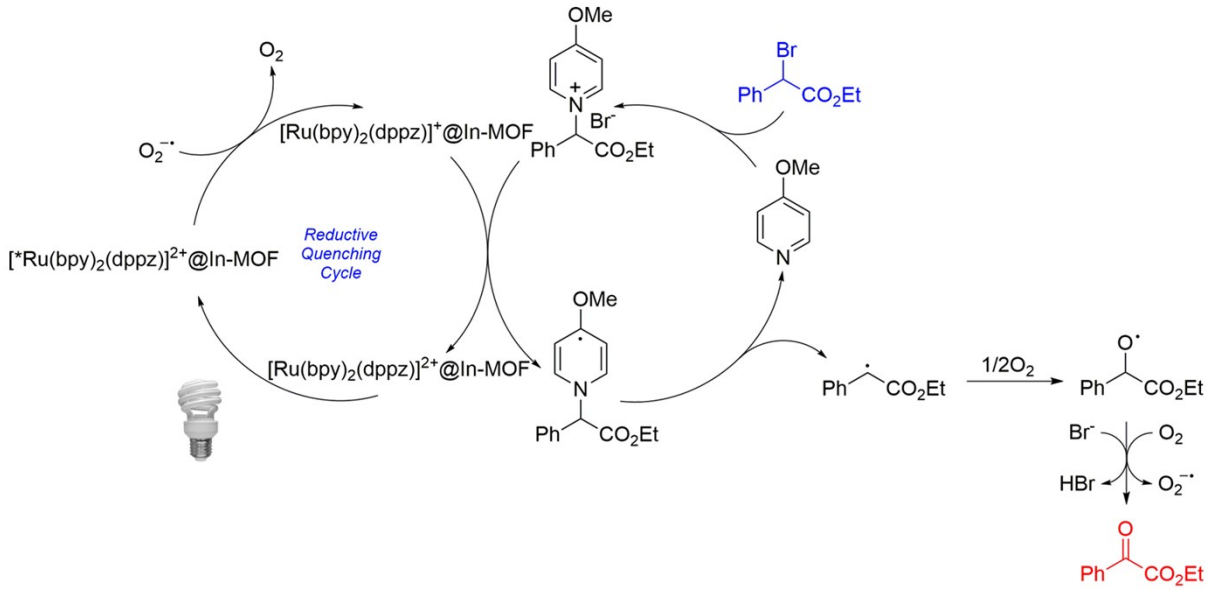

Fig. S10 A proposed reaction mechanism of visible-light driven aerobic oxidation of ethyl α-bromophenylacetate catalyzed by Ru(bpy)$_2$(dppz)@In-MOF in the presence of 4-methoxypyridine [9].

References

[1] E. Amouyal, A. Homsi, J.-C. Chambron and J.-P. Sauvage, *J. Chem. Soc. Dalton Trans*., 1990, 1841–1845.

[2] E.-Y. Cho, J.-M. Gu, I.-H. Choi, W.-S. Kim, Y.-K. Hwang, S. Huh, S.-J. Kim and Y. Kim, *Cryst. Growth Des*., 2014, **14**, 5026−5033.

[3] Y. Huang, Z. Lin, H. Fu, F. Wang, M. Shen, X. Wang and R. Cao, *ChemSusChem*, 2014, **7**, 2647–2653.

[4] Z. Li and C.-J. Li, *J. Am. Chem. Soc*., 2005, **127**, 6968–6969.

[5] A. E. Friedman, J.-C. Chambron, J.-P. Sauvage, N. J. Turro and J. K. Barton, *J. Am. Chem. Soc*., 1990, **112**, 4960−4962.

[6] E. Villani, K. Sakanoue, Y. Einaga, S. Inagi and A. Fiorani, *J. Electroanal. Chem*., 2022, **921**, 116677.

[7] W. E. Jones, Jr. and M. A. Fox, *J. Phys. Chem*., 1994, **98**, 5095−5099.

[8] C. K. Prier, D. A. Rankic and D. W. C. MacMillan, *Chem. Rev*., 2013, **113**, 5322−5363.

[9] Yijin Su, Liangren Zhang and Ning Jiao, *Org. Lett*., 2011, **13**, 2168–2171.